BUTTERWORTH HEINEMANN

Polymer Vol. 36 No. 12, pp. 2363–2369, 1995

0032-3861/95/$10.00+0.00

Non-linear viscoelastic performance of Nomex, Kevlar and polypropylene fibres in a single step stress relaxation test: 2. Moduli, viscosities and isochronal stress/strain curves

F.-J. Wortmann* and K. V. Schulz
Deutsches Wollforschungsinstitut, Veltmanplatz 8, D-52062 Aachen, Germany
(Received 22 June 1993; revised 17 June 1994)

The investigation of the single step stress relaxation behaviour of three polymer fibres, namely Nomex, Kevlar and polypropylene, differing widely in their mechanical properties, shows that a consistent systemization can be applied on the basis of a two-component (TC) model. The model comprises a relaxation function, based on the cumulative log-normal distribution, with a shape that is independent of the type of material and of the strain level. The limits of linearity for viscoelastic behaviour in stress relaxation are deduced and the specific sources of non-linear effects are discussed. For each of the fibres the applicability of simpler models, related to thermorheologically simple or complex materials, is discussed. The results deduced for the stresses and moduli of the elastic and viscous components of the model are plausibly explained on the basis of current models for the fibre structures. The changes of the mean relaxation times with strain are consistent with a solid/fluid transition in an amorphous 'matrix' component initiated at the yield point for Nomex and polypropylene fibres and with the more 'metal-like' nature of Kevlar.

(Keywords: stress relaxation; non-linear viscoelasticity; aramid fibres)

INTRODUCTION

The theory of linear viscoelasticity (LVE) for polymers, similar to Hooke's law for elastic materials, is only an approximation of the real material performance. The range of LVE, extending for glassy polymers over comparatively small stresses and strains[1], is generally the range for the application of polymers as engineering materials. Strains outside the range of LVE, i.e. beyond $\sim 0.5\%$ for semicrystalline, glassy polymers[1], are considered as critical for engineering applications, since the region of non-linear viscoelasticity borders on that of material failure[2]. To further the understanding of the role of strain for the non-linear viscoelastic (NLVE) performance of polymers, this two-part study[3] is directed at the investigation of the strain-induced NLVE effects in Nomex®, Kevlar® and polypropylene fibres, when undergoing single step stress relaxation tests. These polymers were specifically chosen as examples of materials exhibiting typical types of mechanical behaviour as well as for their technical and economic relevance.

In part 1[3], an analytical model is introduced, based on Schapery's theory[4], which enables the strain dependent performance of the three types of polymer fibres in single step stress relaxation tests to be systematically described. The model consists of an elastic component and a viscous contribution, the time dependence of which is described by a form invariate relaxation function, based on a cumulative log-normal distribution.

To elucidate the performance of the model, *Figure 1* (Figure 16 in ref. 3) shows the master curves for the relaxation functions based on experimental data for the three types of fibres. The master curves are identical in shape and just offset on the log-time axis.

The objective of this paper is to discuss the consequences of the application of the two-component (TC) model with respect to the strain dependence of the elastic moduli of the components, of the shift of the relaxation function, as well as of the viscosity of the viscous component. The isochronal stress/strain curves of the components are calculated and discussed with respect to the morphologies of the materials and their possible changes with strain.

EXPERIMENTAL

Kevlar [poly(*p*-phenylene terephthalamide)], investigated in the form of Kevlar 29 (DuPont), is a fibre with a high degree of orientation and crystallinity, that is spun from a liquid crystalline solution of extended chain molecules. As a result, Kevlar is an example of a highly elastic polymeric fibre with a high elastic modulus ($E = 73.3$ GPa), a high breaking stress ($\sigma_B = 2450$ MPa) and a low breaking strain ($\varepsilon_B = 2.9\%$)[3]. Though the chemical structure of Nomex [poly(*m*-phenylene isophthalamide)] (DuPont) is similar to that of Kevlar, the *meta* links of the monomeric unit hinder a high degree of structural organization.

* To whom correspondence should be addressed

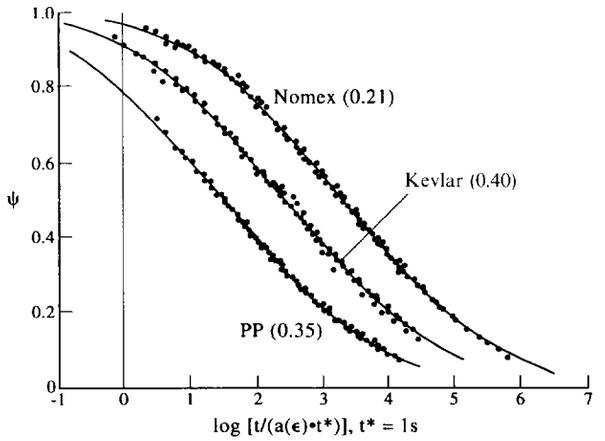

Figure 1 Values for the relaxation function (Ψ) derived from experimental data for the three types of fibres, superimposed to form master curves for the reference strain as given in parentheses. $a(\varepsilon)$ is the acceleration factor given by equation (3)[3]

Consequently, Nomex fibres show the qualitative stress/strain behaviour typical for partially crystalline, glassy polymers ($E=13.7$ GPa, $\sigma_B=502$ MPa, $\varepsilon_B=34\%$)[3]. With a glass transition temperature (T_g) of $\cong 350$°C Nomex is at room temperature far within the glassy region of mechanical behaviour. The polypropylene fibres are a commercial, isotactic product used for textile purposes (Vestolen P1200, Chem. Werke Hüls AG) ($E=1.65$ GPa, $\sigma_B=258$ MPa, $\varepsilon_B=151\%$)[3]. Isotactic polypropylene is a thermoplastic, partially crystalline hydrocarbon polymer, with a T_g ($\cong -10$°C) well below room temperature.

The data given above only refer to the specific fibres used in this study. The experimental aspects of conducting single step stress relaxation tests and of determining fibre strain as well as strain corrections are described in detail in part 1[3].

METHOD OF ANALYSIS

The analysis of the stress relaxation curves is based on a TC model, as implied in the theory of LVE[5], extended for application at strains outside the LVE range by applying Schapery's theory[4] as:

$$E(t,\varepsilon)=h_e(\varepsilon)E^R_\chi+h_v(\varepsilon)\Delta E^R\Psi[t/a(\varepsilon)] \quad (1)$$

E^R_χ and ΔE^R are the limiting moduli of the elastic and viscoelastic components of the TC model at a reference strain, usually chosen to be within the LVE strain range. h_e and h_v are the strain functions that describe the strain dependence of the moduli with respect to the reference. $\Psi(t)$ is the stress relaxation function described here by using the cumulative log-normal distribution (CLND) function given for the $\log_{10}$ time-scale by:

$$\Psi(t)=1/(\sqrt{2\pi}\beta)\int_{\log t}^{\infty}\exp\{-1/2[(x-\alpha)/\beta]^2\}\,dx \quad (2)$$

where x is the integration variable, and α the mean and β the standard deviation of the underlying log-normal distribution[3].

On the basis of this description the acceleration factor $a(\varepsilon)$ in equation (1) is given by:

$$\log a(\varepsilon)=\alpha(\varepsilon^R)-\alpha(\varepsilon) \quad (3)$$

where $\alpha(\varepsilon)$ and $\alpha(\varepsilon^R)$ are the mean log-relaxation times at a given strain, ε, and at the chosen reference strain, ε^R, respectively.

The model represented by equations (1) and (2) can be fitted to transformed, experimental data by means of a weighted linear regression combined with an optimization procedure. The optimization works on the basis of being restricted to a fixed value for the standard deviation in equation (2), namely to $\beta=1.9$. The choice of this value is based on Kubat's investigations[6,7] on the material invariance of the shape of the relaxation function for different polymers and metals. For the present case, the choice for the value of β as well as the assumption of its material—and strain—independence is justified in view of the quality of the master curves in *Figure 1*, which are identical in shape for all fibre materials and only displaced along the log-time axis.

ALTERNATIVE MODELS

Equation (1) comprises a number of simpler models. Tobolsky[8] assumes that time and strain are separable to an extent, that only the magnitude of the modulus is changed by the strain while the location of the relaxation on the log-time-scale remains unaffected, so that:

$$E(t,\varepsilon)=h(\varepsilon)E^R\Psi(t) \quad (4)$$

This model implies that on a $\log E$ *versus* $\log t$ scale the relaxation curves can be superimposed to form a master curve by rigid vertical shifts. This approach works well for the description of the large strain stress relaxation of polymers in the rubbery state[9] and is analogous to that developed by Leaderman[10] for the systemization of the creep compliance curves of mechanically conditioned textile fibres.

Bauwens[11], for analysing the non-linear creep of glassy polymers, basically assumes a performance analogous to the thermorheologically simple materials. Strain leads to a change of the structural temperature that affects only the position of the relaxation function, so that:

$$E(t,\varepsilon)=E^R\Psi[t/a(\varepsilon)] \quad (5)$$

This approach has previously been applied by Passaglia and Koppehele[12] for the systemization of the influence of strain on the relaxation performance of cellulose monofilaments, and more recently by Tieghi *et al.*[13] for poly(methyl methacrylate) sheets. The equivalence of stress or strain and temperature led Bergen[14] to propose the use of stress as a reduced variable in creep experiments rather than temperature to predict the long-term performance of thermoplastic engineering materials.

A combination of equations (4) and (5) yields:

$$E(t,\varepsilon)=h(\varepsilon)E^R\Psi[t/a(\varepsilon)] \quad (6)$$

This description relates to that for thermorheologically complex materials, where the curves may be superimposed on a log–log scale by horizontal and vertical shifts. Schapery[4] suggests the analogous approach to be applied for the time–temperature superposition for semi-crystalline polymers, where the horizontal shift factor primarily reflects the temperature dependence of the amorphous regions, while the vertical shift accounts for the change in the rigidity of the crystalline regions. Behaviour in accordance with equation (6) was observed

by Nagamatsu *et al.*[15] for the relaxation performance of polyethylene.

Assuming equal strain functions for both components and strain independence for the form of the relaxation function, a simplified form of equation (1), namely:

$$E(t,\varepsilon)=h(\varepsilon)\{E_{\chi}^{R}+\Delta E^{R}\Psi[t/a(\varepsilon)]\} \qquad (7)$$

has successfully been applied for a systematic description of the NLVE stress relaxation performance of wool fibres[16], where equation (7) in this specific case is justifiable in a straightforward manner on account of the morphology of α-keratin fibres.

All of these models, however, imply that the shape of the relaxation function and hence of the normalized relaxation time spectrum remains unaffected by the strain level. This is in contrast to the observation by Yee[17] of a narrowing of the spectrum with strain for the stress relaxation of polycarbonate, while Dean *et al.*[18] observed a broadening of the retardation time spectrum with stress for the creep performance of poly(vinyl chloride). Finally, it is important to note that no effort was made to implement the method of multiple integral functional relationships[19] for the analysis of the results.

RESULTS AND DISCUSSION

Nomex

The fit of equations (1) and (2) to the experimental data leads to the determination of the properties of the two components of the TC model, namely of E_{χ}, ΔE and χ. *Figure 2* shows the values of the moduli *versus* strain. The solid lines are just heuristic graphical descriptions, used for the sake of clarity. A log scale was used for strain to provide a higher resolution of the data at low strains.

In the low strain region ($\varepsilon \gtrsim 1\%$) E_{χ} exhibits a constant level estimated as ≈ 7 GPa, while ΔE continuously increases to reach a maximum of ≈ 6 GPa around 1% strain, dropping off at higher strains. These characteristic moduli for the elastic and viscous components may be chosen as values for E_{χ}^{R} and ΔE^{R} in equation (1), giving the values of $h_{e}(\varepsilon)=E_{\chi}(\varepsilon)/E_{\chi}^{R}$ and $h_{v}(\varepsilon)=\Delta E(\varepsilon)/\Delta E^{R}$. The relative contributions of E_{χ}^{R} and ΔE^{R} to the overall reference fibre modulus, $E_{0}^{R}=E_{\chi}^{R}+\Delta E^{R}$, are $\approx 55\%$ and $\approx 45\%$, respectively.

The mean of the CLND function, α, the values of which are summarized for all materials in *Figure 3*, shows for

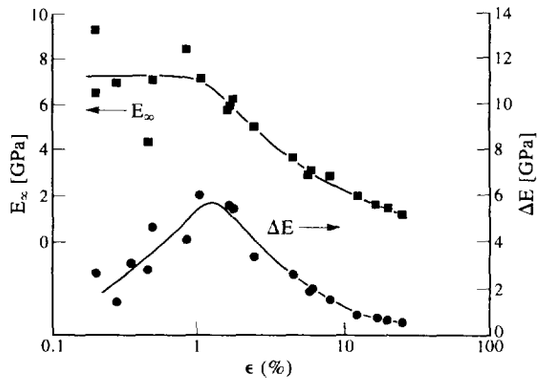

Figure 2 Limiting moduli of the elastic and viscous components in Nomex (E_{χ} and ΔE, respectively) *versus* strain

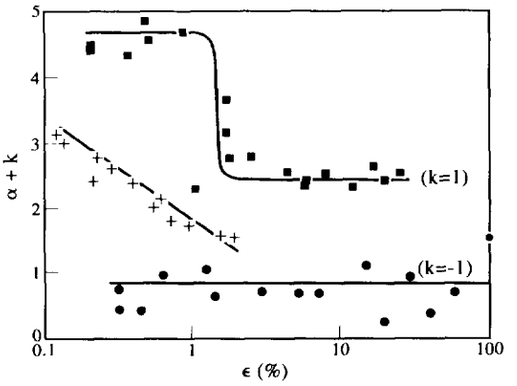

Figure 3 Mean log-relaxation times α for (■) Nomex, (+) Kevlar and (●) polypropylene fibres *versus* strain. The curves for Nomex and polypropylene are displaced vertically by a constant, *k*, given in parentheses, for the sake of clarity

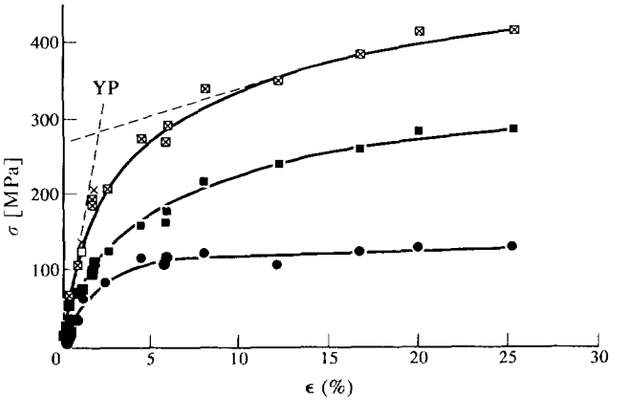

Figure 4 Experimental and isochronal stress/strain curves for Nomex fibres and of the components of the TC model (see text). YP, yield point. (■) σ_{χ}; (●) $\Delta\sigma$; (×) σ_{0}; (□) $\sigma(0)$

Nomex a pronounced shift by two decades between 1% and 2% strain from $\alpha=3.5_{5}\pm0.1_{9}$ (95% confidence limits, $\varepsilon<1\%$) to $\alpha=1.4_{7}\pm0.0_{9}$ for strains beyond 4%. The position of the shift coincides with the strain level where the moduli show a change in behaviour and with the yield point of the material, that may be constructed by linear extrapolation of the $\sigma(0)$ *versus* ε data for low and high strains, as indicated by the broken lines in *Figure 4*. $\sigma(0)$ is the initial stress at the end of the straining step, so that $\sigma(0)$ *versus* ε represents the experimental stress/strain curve.

The results summarized in *Figures 2* and *3* show that linearity, i.e. independence of strain, resides in E_{χ} and α, where the threshold strain of $\approx 1\%$ coincides very well with the LVE strain limits given by Yannas[1] for glassy, amorphous polymers (1%), while it greatly exceeds the common values for semicrystalline polymers (0.1–0.4%[1], 0.01–0.03%[5]). The data for ΔE show deviations from strain independence for the whole strain range investigated so that from a formal point of view, Nomex exhibits no region of LVE behaviour in our experiments. However, the results may not be inconsistent with the assumption of linearity for the range of strains of $\varepsilon \lesssim 0.1\%$. Furthermore, the overall performance of Nomex is consistent with an effective, approximate LVE behaviour

for a strain range of up to 0.5%, due to the scatter of the data for ΔE in this range.

For higher strains ($\varepsilon > 10\%$), α is constant and E_α and ΔE tend to level off. In this region, where the experiment basically realizes relaxation from continuous flow (*Figure 4*), linearity in modulus and relaxation time is again approached. Due to the strain independence of α the behaviour for the viscous component alone is well described by the Tobolsky model [equation (4)].

Relating the components of the TC model to the elastic response of the morphological components of the polymer, namely E_α to an elastic, crystalline structure and ΔE to an amorphous, glassy 'matrix' component, the obvious differences in the NLVE behaviour of the components correspond to the observation by Yannas[1] that, for example, for polycarbonate non-linearity appears at a strain of 1.1% in purely mechanical tests, while this non-linearity is not shown below 3.4% when opto-mechanical methods are used.

For a viscoelastic solid, the fluid part of the behaviour is described by a viscosity parameter η as[5]:

$$\eta = \Delta E \int_{-\alpha}^{+\alpha} t\Psi(t)\, \mathrm{d} \ln t \qquad (8)$$

Assuming the normalized relaxation time spectrum, $h(\tau)$, to follow a log-normal distribution, Stootman[20] derived an expression for η:

$$\eta = \Delta E 10^{(\beta^2/2 + \alpha)} t^* \qquad (t^* = 1\ \mathrm{s}) \qquad (9)$$

Applying Alfrey's rule[21] the log-normally distributed $h(\tau)$ leads to the CLND function for $\Psi(t)$, so that equation (9) may be taken as a good estimate for the elongational steady-flow viscosity of the viscous component based on equations (1) and (2), modified for the case of NLVE behaviour:

$$\eta = \Delta E(\varepsilon) 10^{[\beta^2/2 + \alpha(\varepsilon)]} t^* \qquad (10)$$

By introducing the strain function $h(\varepsilon)$ and the shift factor $a(\varepsilon)$ the normalized form is obtained:

$$\eta = h_\nu(\varepsilon) \Delta E^R 10^{[\beta^2/2 + [\alpha^R - \log a(\varepsilon)]]} t^* \qquad (11)$$

Figure 5 summarizes the viscosity of the viscous component of the Nomex fibres *versus* strain. For low strains below the yield point the viscous component exhibits a viscosity in the range of $1\text{–}3 \times 10^{17}$ Pa s, slightly increasing with strain due to the related change of ΔE (*Figure 2*). The values greatly exceed $\eta = 10^{14}$ Pa s, which is the value generally used to distinguish between soft solids and highly viscous fluids, and are in agreement with the pronounced glassy character of Nomex at room temperature. Beyond the yield point the viscosity decreases discontinuously by two orders of magnitude due to the combined effects of the decreases in ΔE and α and reaches the range of $10^{14.5}\text{–}10^{15.5}$ Pa s (*Figure 5*), which approaches the range characteristic for highly viscous fluids. This result supports the view that the yield point marks a strain-induced glass transition, i.e. a solid/fluid transition[22,23].

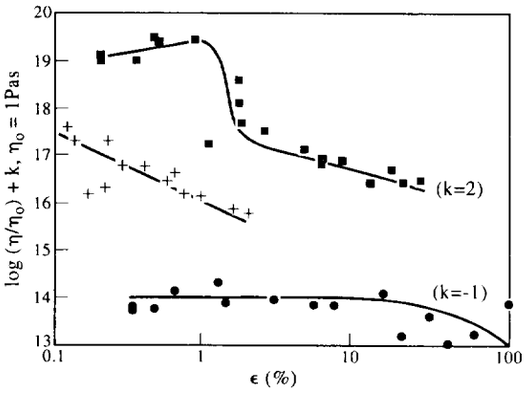

Figure 5 Elongational steady-flow viscosity η of the viscous component of (■) Nomex, (+) Kevlar and (●) polypropylene fibres *versus* strain. The curves for Nomex and polypropylene are displaced vertically by a constant, k, given in parentheses, for the sake of clarity

From the fit of $\Psi(t)$ to the experimental data[3], the various moduli and hence the equilibrium stress of the elastic component, $\sigma_\alpha = E_\alpha \varepsilon$, the limiting elastic stress of the viscous component, $\Delta\sigma$, and the true initial stress, $\sigma_0 = \sigma_\alpha + \Delta\sigma$, are determined, so that for each of the components of the TC model the isochronal ($t = 0$) stress/strain curve can be constructed. These curves are summarized in *Figure 4* together with the data for the experimental stress/strain curve, $\sigma(0)$ *versus* ε. The curves show distinct similarities, with the yield point being more pronounced for $\Delta\sigma$ than for σ_α. The results for σ_0 and $\sigma(0)$ largely coincide, showing that during yielding very little relaxation occurs, this being consistent with the high viscosity of the viscous component even at strains beyond the yield point.

Connecting σ_α with the mechanical performance of a potentially elastic phase in Nomex, the stress/strain curve of the elastic component of the TC model is in qualitative agreement with the structural, microfibrillar model of Peterlin[24] for drawn, semicrystalline fibrous polymers. In this model elongation proceeds by shear displacement of adjacent, semicrystalline fibrils and by the unfolding of chains from crystal blocks therein. The process is initiated at the yield point and from thereon continues for Nomex at an increasing stress level, where, however, the rate of stress increase decreases with increasing strain (*Figure 4*). Beyond the yield point around 4% strain $\Delta\sigma$ attains a largely constant value (119 ± 2 MPa), which is consistent with the relaxation of an amorphous matrix component in Nomex proceeding from continuous flow.

Equation (1) represents a rather complex model, and it is of interest to determine to what extent it may be simplified in terms of equations (4)–(7), while still serving as a reasonable basis for the systemization of the relaxation curves.

The applicability of equation (4) requires, in contrast to equations (5)–(7), the constancy of α. This condition is satisfied for Nomex for strains below 1% and above ~2% strain, respectively (*Figure 3*). To be able to superimpose the related relaxation curves by purely vertical shifts on the log–log scale further requires, in the view of equation (1), a constant ratio of the component moduli ($E_\alpha/\Delta E$). This ratio is plotted in *Figure 6 versus* strain for the three types of fibres, showing that for Nomex this condition is only satisfied for strains beyond 10%. This coincides with the observations by Tobolsky[8] and Leaderman[10] on the validity of equation (4) for rubber and textile fibres, respectively, at high strains. For strains between 2% and 10%, where ($E_\alpha/\Delta E$) only changes between ≈ 1.5 and ≈ 2.2, equation (4) may still be considered as an approximation, thus conceding

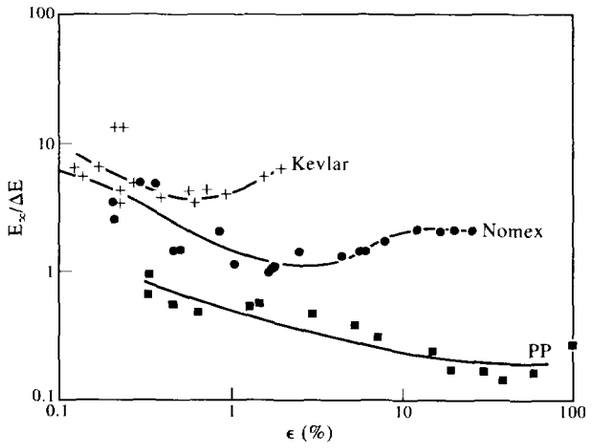

Figure 6 Ratio of the component moduli (E_∞, ΔE) *versus* strain for the three types of fibres

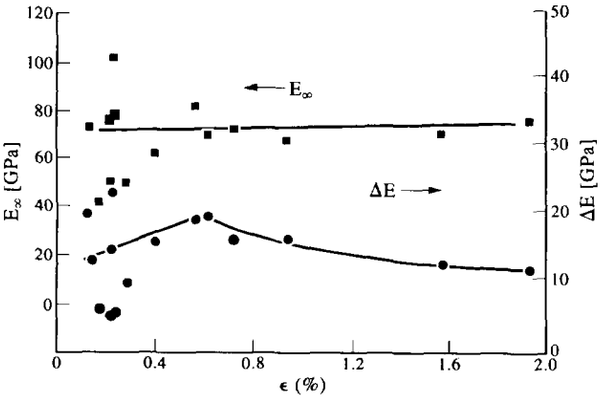

Figure 7 Limiting moduli of the elastic and viscous components in Kevlar (E_∞ and ΔE, respectively) *versus* strain

approximate validity of its inherent principles for Nomex for strains beyond the yield point.

However, just from a purely subjective judgement of the experimental curves on the $\log E$ *versus* $\log t$ scale[3], it appears that it would be difficult to justify the choice of equations (4), (5) or (6) for the systemization of the data.

Kevlar

Figure 7 plots E_∞ and ΔE *versus* ε for Kevlar fibres in the strain range of ~0.2–2%. Below around 0.6% strain the data show a considerable random scatter that is obviously 'pulled out' at higher strains. The scatter of the moduli at low strains is attributed to inter- and intrafibre variations of structural orientation that are levelled out on straining. Such variations have been detected in the light scattering profiles of Kevlar 49 fibres[25] and are rather typical for fibrous polymers[26].

Around 0.6% strain E_∞ attains a constant level of $E_\infty^R = 71$ GPa, while ΔE has increased up to a value of $\Delta E^R = 19.5$ GPa and continuously decreases from thereon to approach a level around $\Delta E = 11.4$ GPa ($\varepsilon = 2\%$), equivalent to $h_\nu = 0.58$. The increase of ΔE in the region of low strains is in good agreement with the experimental results of Ericksen[27], who observed an increase in the Young's modulus of Kevlar 29 fibres for small creep strains ($\varepsilon = 0.18$–0.38%). Though the contribution of the viscous component to the overall modulus in the reference state (22%) is, as expected, considerably lower for Kevlar compared to Nomex, the size of the contribution is nevertheless surprising in the view of the generally assumed 'elasticity' of Kevlar. The critical strain level of 0.6% for ΔE agrees well with the level of ~0.5% where Allen and Roche[28] observe a decrease of modulus in the first derivative of the stress/strain curves for Kevlar 29 fibres.

In contrast to Nomex, where α stays constant for strains below ~1.5%, α already drops for Kevlar for this small strain range linearly with log-strain by 1.5 orders of magnitude (*Figure 3*), which is comparable in size to the overall effect for Nomex for a much larger strain range. This pronounced decrease of the mean relaxation time contributes, together with the decrease of ΔE beyond 0.6% strain, to the observation of irreversible deformation of Kevlar fibres on cyclic loading, increasing in magnitude beyond the threshold strain of 0.5%[28].

Since ΔE shows no drastic changes with strain the viscosity change is largely governed by the change in α and consequently changes virtually linearly with log-strain from a level of $10^{17.5}$ to $10^{15.5}$ Pa s (*Figure 5*), thus also approaching the range of highly viscous fluids.

Compared to Nomex the formal deviation from LVE behaviour is even more pronounced in Kevlar where linearity with strain may only be detected for E_∞, so that, in agreement with literature data[28], even for low strains no LVE behaviour can be expected.

The linear shift of α with log-strain is not only characteristic for Kevlar but also for Technora®, and shows a similarity to the NLVE performance of steel at elevated temperatures[29]. This result might be taken as a basis for the hypothesis that in Kevlar relaxation proceeds by a mechanism analogous to grain boundary slippage in metals[30], rather than by molecular movements. The material invariance of the shape of the relaxation function would, furthermore, let the validity of any molecular, viscoelastic mechanisms for aramid fibres derived from the shape of their relaxation or creep curves[31] appear questionable. The suggested differences in the morphological origin of the relaxation phenomenon for Nomex and Kevlar is covered by Zener's hypothesis[32] that the interface between crystals may reasonably be expected to have the characteristics associated with amorphous materials.

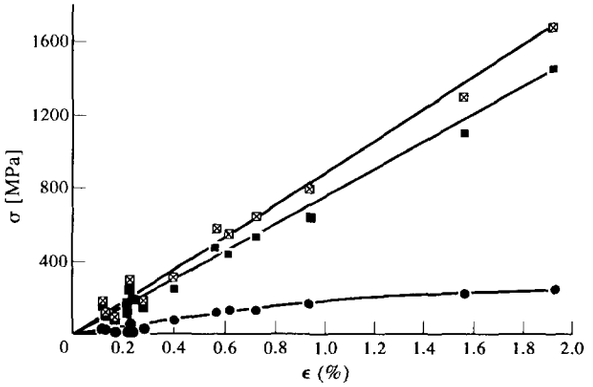

Figure 8 Experimental and isochronal stress/strain curves for Kevlar fibres and of the components of the TC model. (■) σ_∞; (●) $\Delta\sigma$; (×) σ_0; (□) $\sigma(0)$

The isochronal stress/strain curves for Kevlar (*Figure 8*) show negligible stress loss during straining and pronounced linearity for $\sigma_0(\varepsilon)$ and $\sigma_\chi(\varepsilon)$. Only $\Delta\sigma$ shows on close inspection an S-shaped appearance at low strains and a tendency to level out beyond 1% strain. This performance of $\Delta\sigma$ with strain is consistent with the non-linear stress/strain curves of Kevlar fibres observed by Ericksen[27] and Allen *et al.*[33], thus identifying the viscous component in aramids as the source of this non-linearity.

The molecular orientation response to deformation is well established for Kevlar fibres[28]. From a morphological point of view the non-linear stress/strain curve is attributed to the opening up and orientation under load of the Kevlar fibre's pleated supermolecular structure[33]. On a more specific, though simplified level $\sigma_\chi(\varepsilon)$ and $\Delta\sigma(\varepsilon)$ may in certain aspects be related to the mechanisms proposed by Ericksen[27] for the response of adjacent crystallites in Kevlar to strain, though this aspect will require further investigations.

Checking simplifications of the data systemization via equations (4)–(7) shows that equation (4) will be inapplicable due to the pronounced change of α with strain. Equation (5) requires the constancy of E^R with strain and, in the view of results by Guimaraes and Burgoyne[34] on the creep of aramid ropes, may be considered as a good approximation, in view of the constancy of E_∞ with strain and the comparatively small contribution of ΔE. However, this would be inconsistent with the experimental observation that the creep rate of aramid yarns and fibres increases with stress[27,35], so that for the related modulus the application of equation (6) would be required, i.e. vertical and horizontal superposition in a log E *versus* log t plot. *Figure 6* shows that due to the virtual constancy of the moduli ratio within experimental scatter, equations (6) and (7) would be satisfactory descriptions in the range between ~0.2% and 1% strain. However, inspection of the experimental curves of this study in a log–log plot (Figure 5 in ref. 3) as well as of literature data[34] reveals that the choice of the appropriate superposition procedure, based only on the appearance of the raw data, would be anything but unambiguous.

Polypropylene

Figure 9 plots E_χ and ΔE *versus* ε for polypropylene fibres. Despite the rather substantial, though not atypical[26], scatter of the moduli at low strains ($\varepsilon \leqslant 1\%$), the values indicate a constancy of both component moduli at levels

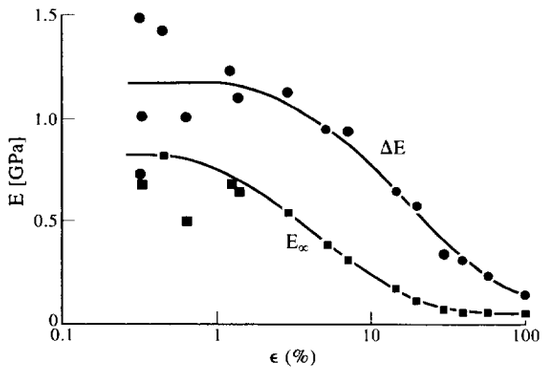

Figure 9 Limiting moduli of the elastic and viscous components in polypropylene fibres (E_χ and ΔE, respectively) *versus* strain

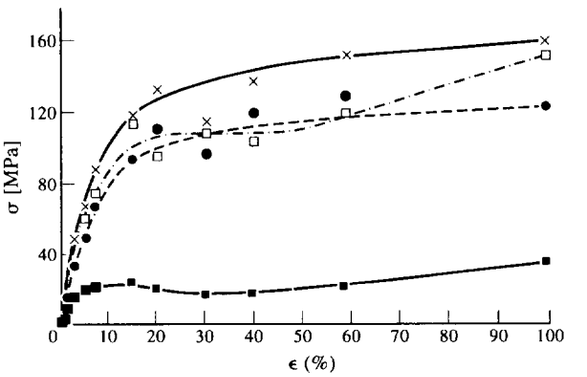

Figure 10 Experimental and isochronal stress/strain curves for polypropylene fibres and of the components of the TC model. (■) σ_χ; (●) $\Delta\sigma$; (×) σ_0; (□) $\sigma(0)$

of $E^R_\chi \cong 0.8$ GPa and $\Delta E^R \cong 1.2$ GPa. The relative contributions are 40% and 60% for the elastic and viscous components, respectively. Beyond 1% strain the scatter is removed and both moduli decrease to reach values at 100% strain that are about one order of magnitude lower, showing similar behaviour to Nomex.

The mean of the CLND function, α, is observed to be independent of strain over the whole range between 0.2% and 100% strain (*Figure 3*). This performance is in pronounced contrast to that of Nomex and Kevlar and thus rather surprising at first sight. It becomes plausible, however, in view of the theory that strains beyond the yield point initiate a strain-induced glass transition. Such a transition is observed for Nomex (*Figure 3* and *5*), which at room temperature is well below the glass transition temperature, and is consequently absent for polypropylene, which at room temperature is well above the glass transition temperature and where the viscosity of the viscous component already at low strains is well within the range of highly viscous fluids ($\eta_{1\%} \cong 10^{15}$ Pa s, *Figure 5*). As a consequence of the constancy of α the viscosity drops under the influence of the decrease of $\Delta E(\varepsilon)$ only by one order of magnitude from $\approx 10^{15}$ to $\approx 10^{14}$ Pa s.

Figure 10 plots the experimental and isochronal stresses for polypropylene fibres *versus* strain. $\sigma(0)$ shows the characteristic yield point around 10% strain and a plateau region up to ~50% strain. The difference between σ_0 and $\sigma(0)$ is a result of the relaxation proceeding during straining.

As for Nomex, the behaviour of the components of the TC model may be related to the performance of the morphological components, namely $\Delta\sigma$ can be related to that of the amorphous and σ_χ can be related to that of the crystalline component, or, according to the Peterlin model[24], rather to the semicrystalline filaments.

$\Delta\sigma$ increases continuously with strain, levelling off beyond the yield point to the strain invariate stress level of continuous flow (≈ 120 MPa). This performance is analogous to $\Delta\sigma(\varepsilon)$ for Nomex.

σ_χ may be assumed to reflect the stress/strain characteristics of the strain induced shear displacement mechanism in the stacked-lamellar structure of the fibrils. The curve for $\sigma_\chi(\varepsilon)$ shows a maximum around the yield point that is typical for so-called 'strain softening' polymers, thus identifying the performance of the fibrillar phase as the source for this effect and for the plateau formation in the fibre stress/strain curve. The dis-

similarities between the filament stress/strain curves for polypropylene and Nomex may be related to the differences between the models discussed by Prevorsek *et al.*[37] for the analysis of structure/property relationships of polyethylene and polypropylene on the one hand and aliphatic polyamides and poly(ethylene terephthalate) on the other.

From the point of view of LVE behaviour, polypropylene fibres are an ideal material compared to Nomex and Kevlar. Due to the virtual constancy of all three variables in equation (1) for small strains, LVE behaviour is observed up to the classical limit of 1% strain, usually only assumed to be valid for amorphous, glassy polymers[1].

Due to the strain independence of α the first choice for a superposition rule for the relaxation curves is equation (4). To check the inherent assumption of a constant ratio of the component moduli, the values of $E_\alpha/\Delta E$ for polypropylene are summarized in *Figure 6*. The results show that the ratio decreases continuously at strains between 1% and 10%, levelling off beyond the yield point. Similarly as in Nomex, equation (4), originally applied for large strain relaxation of polymers in the rubbery state[9], is hence a good approximation for the systemization of the curves for relaxation from continuous flow for semicrystalline polypropylene fibres. The consideration of the performance of the variables of the TC model hence rationalizes the applicability of an appropriate, approximate superposition method, the choice of which would, again, have been rather ambiguous on simple inspection of the experimental data[3].

CONCLUSIONS

It appears that the application of the TC model, as presented here, leads to a systemization of the relaxation curves that shows a high degree of accuracy and consistency and also plausibility for the interpretation of the phenomena that control the viscoelastic performance, on a morphological as well as a molecular, though unspecific, level.

ACKNOWLEDGEMENTS

The authors gratefully acknowledge the financial support of this investigation by the Deutsche Forschungsgemeinschaft (DFG) within the framework of the Sonderforschungsbereich 332 and also by the Ministerium für Wissenschaft und Forschung des Landes Nordrhein-Westfalen.

REFERENCES

1 Yannas, I. V. *J. Polym. Sci. Macromol. Rev.* 1974, **9**, 163
2 Menges, G. 'Werkstoffkunde der Kunststoffe', 2nd Edn, Hanser Verlag, Munich, 1984
3 Wortmann, F.-J. and Schulz, K. V. *Polymer* 1994, **35**, 2108
4 Schapery, R. A. *Polym. Eng. Sci.* 1969, **9**, 295
5 Ferry, J. D. 'Viscoelastic Properties of Polymers', 2nd Edn, Wiley, New York, 1970
6 Kubat, J. *Nature* 1965, **205**, 378
7 Kubat, J. 'A Similarity in the Stress Relaxation Behaviour of High Polymers and Metals', Acoprint, Stockholm, 1965
8 Tobolsky, A. V. in 'Polymer Science and Materials' (Eds A. V. Tobolsky and H. F. Mark), R. E. Krieger, New York, 1980, Ch. 10
9 Halpin, J. C. *J. Appl. Phys.* 1965, **36**, 2975
10 Leaderman, H. 'Elastic and Creep Properties of Filamentous Materials and other High Polymers', The Textile Foundation, Washington, DC, 1943
11 Bauwens, J. C. *Colloid Polym. Sci.* 1992, **270**, 537
12 Passaglia, E. and Koppehele, H. P. *J. Polym. Sci.* 1958, **33**, 281
13 Tieghi, G., Fallini, A. and Levi, M. *Polym. Commun.* 1991, **32**, 245
14 Bergen, R. L. *Plast. Eng.* 1967, **23**, 57
15 Nagamatsu, K., Takemura, T., Yoshitomi, T. and Takemoto, T. *J. Polym. Sci.* 1958, **33**, 515
16 Wortmann, F.-J. and DeJong, S. *J. Appl. Polym. Sci.* 1985, **30**, 2195
17 Yee, A. F. *J. Polym. Sci., Polym. Phys. Edn* 1988, **26**, 2463
18 Dean, G. D., Read, B. E., Lesniarek-Hamid, J. L. and Tomlins, P. E. *Plast. Rubber Comp. Proc. Appl.* 1992, **17**, 225
19 Findley, W. N., Lai, J. S. and Onaran, K. 'Creep and Relaxation of Nonlinear Viscoelastic Materials', North Holland, Amsterdam, 1976
20 Stootman, F. *PhD Thesis*, University of NSW, Sydney, 1977
21 Alfrey, T. and Doty, P. *J. Appl. Phys.* 1945, **16**, 700
22 Shay, R. M. and Caruthers, J. M. *J. Rheol.* 1986, **30**, 781
23 Nanzai, Y. *J. Non-Cryst. Solids* 1991, **131–133**, 516
24 Peterlin, A. in 'The Strength and Stiffness of Polymers' (Eds A. E. Zachariades and R. S. Porter), Marcel Dekker Inc., New York, 1983, Ch. 3
25 Roche, E. J., Allen, S. R., Finder, C. R. and Paulson, C. *Mol. Cryst. Liq. Cryst.* 1987, **153**, 547
26 Schoppee, M. M. and Skeleton, J. *J. Appl. Polym. Sci. Appl. Polym. Symp.* 1991, **47**, 301
27 Ericksen, R. H. *Polymer* 1985, **26**, 733
28 Allen, S. R. and Roche, E. J. *Polymer* 1989, **30**, 996
29 Wortmann, F.-J. and Schulz, K. V. *Makromol. Chem. Macromol. Symp.* 1991, **50**, 55
30 Kröner, E. *Rheol. Acta* 1973, **12**, 374
31 Rogozinsky, A. K. and Bazhenov, S. L. *Polymer* 1992, **33**, 1391
32 Zener, C. 'Elasticity and Anelasticity of Metals', University of Chicago Press, Chicago, 1948
33 Allen, S. R., Roche, E. J., Bennett, B. and Molaison, R. *Polymer* 1992, **33**, 1849
34 Guimaraes, G. B. and Burgoyne, C. J. *J. Mater. Sci.* 1992, **27**, 2473
35 Wang, J. Z., Dillard, D. A. and Ward, T. C. *J. Polym. Sci., Polym. Phys. Edn* 1992, **30**, 1391
36 Prevorsek, D. C., Harget, P. J., Sharma, R. K. and Reimschuessel, A. C. *J. Macromol. Sci. Phys.* 1973, **B8**(1–2), 127